Constraining color-charge effects of partonic energy loss with jet-axis-based inclusive jet substructure measurement

Raghunath Pradhan [*] and Olga Evdokimov [†]
Department of Physics, 845 West Taylor Street, University of Illinois Chicago, Chicago, Illinois 60607, USA

(Received 9 September 2025; accepted 24 November 2025; published 22 December 2025)

This study investigates the color-charge dependence of parton energy loss in the quark-gluon plasma (QGP) medium and the associated relative modifications of quark and gluon jet fractions compared to vacuum, using jet axis decorrelation observables. Recent CMS jet axis decorrelation measurements in PbPb collisions at 5.02 TeV are interpreted using Pythia simulations with varied quark/gluon jet compositions and emulated color-charge dependent energy loss. A template-fit procedure is employed to estimate the limits on gluon jet fractions in the published CMS data and average shift in jet momentum due to quenching for quark- and gluon-initiated jets traversing the QGP. The extracted gluon jet fractions and the estimated quark and gluon energy losses based on this study of jet axis decorrelations are found to be consistent with other model calculations based on inclusive observables. This work illustrates the use of jet substructure measurements for providing constraints on the color-charge dependence of parton energy loss and offers valuable insights for jet quenching models.

DOI: 10.1103/cj9y-mcxj

I. INTRODUCTION

Ultrarelativistic heavy-ion collision experiments aim to recreate a deconfined state of quarks and gluons, known as the quark-gluon plasma (QGP), under laboratory conditions to investigate the properties of this unique form of nuclear matter. Jets, collimated streams of particles produced in high-energy collisions, serve as versatile tools for probing the QGP [1,2]. These jets are initiated by energetic quarks and gluons (partons) produced in high-momentum-transfer processes during the initial stages of the collision. The partons subsequently fragment into lower-energy partons, which then hadronize into final-state particles. As the outgoing partons traverse the QGP, they lose energy through interactions with the medium. These interactions result in medium-induced modifications to various experimental observables, collectively referred to as "jet quenching." Experimental evidence for jet quenching has been observed using multiple probes at both the BNL RHIC [3,4] and the CERN LHC [5–8]. Such probes include the suppression of high transverse momentum (p_{T}) particle yields, modifications to jet fragmentation functions, and changes in jet shapes. Some recent reviews on this subject can be found in Refs. [1,2,9,10].

In parallel with experimental studies of quenching phenomena, significant theoretical advances have been made over the past two decades in characterizing partonic energy loss in the QGP medium. The mechanisms understood as the primary contributors to the energy loss are medium-induced gluon radiation and collisional energy loss. Despite substantial progress on both theoretical and experimental fronts, the details of parton-medium interactions and the precise mechanisms governing parton energy loss remain unclear. Emerging techniques, such as jet substructure studies and the tagging (or selection) of quark and gluon jets, offer new insights into energy loss mechanisms [11,12]. Due to differences in Casimir color factors ($\mathrm{C_F} = 4/3$ for quarks and $\mathrm{C_A} = 3$ for gluons), gluon-initiated jets are expected to interact more strongly with the QGP and lose more energy compared to quark-initiated jets. This enhanced energy loss reduces the fraction of gluon jets within the surviving jet population in heavy-ion collisions at a given jet p_{T} compared to the vacuum case without a medium. Recent measurements suggest that the relative fractions of quark and gluon jets are modified in heavy-ion collisions compared to elementary proton-proton collisions, reflecting the differential energy loss due to the distinct color charges of quarks and gluons [13–16].

The CMS experiment attempted to study gluon-like jet fractions by applying the template-fit method to the jet-charge observable for an inclusive jet sample from lead-lead (PbPb) collisions at a center-of-mass energy per nucleon pair ($\sqrt{s_{\mathrm{NN}}}$) of 5.02 TeV [17]. This measurement found no significant evidence of a decrease in gluon jets or a corresponding increase in quark jets. The jet-charge observable currently lacks theoretical predictions for the expected in-medium modifications. The ATLAS experiment measured the jet nuclear modification factor (R_{AA}) and estimated the fractional energy loss (S_{loss}) for photon-tagged jets and compared these observables with those for inclusive jets [18]. Since photon-tagged jets are dominantly quark-initiated, this comparison provides sensitivity to

[*]Contact author: raghunath.pradhan@cern.ch
[†]Contact author: evdolga@uic.edu

Published by the American Physical Society under the terms of the Creative Commons Attribution 4.0 International license. Further distribution of this work must maintain attribution to the author(s) and the published article's title, journal citation, and DOI. Funded by SCOAP[3].

the color-charge dependence of parton energy loss [18]. It was reported that the R_{AA} of photon-tagged jets is significantly higher, and their estimated S_{loss} significantly lower, than those of inclusive jets, providing evidence that quark jets lose less energy than gluon jets in the medium. However, a detailed description of color-charge dependent energy loss in the QGP medium, along with the relative modifications of quark and gluon jet fractions, remains elusive and warrants further experimental and theoretical investigation through additional observables.

Recently, the CMS experiment measured a new jet substructure observable, the jet axis decorrelation (Δj), for a similar data sample (inclusive jets from 5.02 TeV PbPb collisions) [19]. This observable is predicted to be sensitive to the parton-medium interactions and provide constraints for energy loss models [20]. The study found that Δj is narrower than predictions from various unquenched models, such as PYTHIA [21] and HERWIG [22]. This narrowing could be attributed to modifications in the internal structure of jets caused by interactions with the QGP medium, selection biases favoring less-quenched jets, and/or results from the color-charge dependence of partonic energy loss. In the latter scenario, the larger average energy loss shifts gluon jets further down in energy compared to quark jets, resulting in a different partonic composition of quenched and unquenched jet samples.

In this paper, we attempt to interpret the recent CMS jet axis decorrelation measurements [19] by comparing them to PYTHIA8 [21] simulations with varying relative quark/gluon fractions and emulated color-charge dependent jet energy loss. A template-fit approach is employed to estimate the lower limit on gluon jet fractions within the inclusive jet sample. The quark- and gluon-initiated jet templates are derived from inclusive jet samples in 5.02 TeV pp collisions simulated with the PYTHIA8 event generator. Simultaneously, the average jet energy loss for inclusive, quark, and gluon jets is estimated by minimizing the chi-square (χ^2) between the Δj distributions measured by CMS and those generated by PYTHIA8 with an applied p_T shift imitating energy loss. Two scenarios are considered. First, in a simplistic approximation, all jets are assumed to lose the same fractional energy, with each jet's p_T shifted down by the same fraction of transverse momenta. Additionally, we explore the color-charge dependent energy loss scenario, for which quark and gluon jets are allowed independent shifts to account for their differing energy losses.

The paper is organized as follows. Section II outlines the analysis framework used to measure jet axis decorrelation. Section II A discusses the template fits, while Sec. II B focuses on estimating the p_T shifts for inclusive, quark, and gluon jets to interpret the CMS Δj distributions. Section III presents the results, followed by a detailed discussion. Finally, Sec. IV summarizes the main conclusions of this work.

II. ANALYSIS METHOD AND FRAMEWORK

The jet axis decorrelation, Δj, is the angular difference between the axes determined by the anti-k_T energy-weighted (E-scheme) recombination and the winner-take-all (WTA) recombination schemes [19,20]. It is defined as

$$\Delta \mathrm{j} = \sqrt{(\eta^{\text{E-scheme}} - \eta^{\text{WTA}})^2 + (\phi^{\text{E-scheme}} - \phi^{\text{WTA}})^2}, \quad (1)$$

where $\eta^{\text{E-scheme}}$ (η^{WTA}) and $\phi^{\text{E-scheme}}$ (ϕ^{WTA}) denote the pseudorapidity and azimuthal angle of the E-scheme (WTA) axis, respectively, which characterize the jet's direction. In the E-scheme jet recombination [23], the jet axis is determined by the four-vector sum of its constituent particles, representing a momentum-averaged direction of energy flow that includes contributions from soft particles. This method clusters jets by iteratively combining particle pairs into pseudojets, with the direction of each new pseudojet defined by the vector sum of the four-momenta of its constituents. The final four-vector defines the E-scheme jet axis in (η, ϕ) coordinates. Conversely, the WTA scheme emphasizes the hardest prong at each clustering step, making it more sensitive to collinear radiation. To determine the WTA axis, the jet is reclustered using the WTA algorithm [24,25] with the same constituents, where the direction of each new pseudojet aligns with the highest-p_T particle or pseudojet. This typically results in the WTA axis aligning with the direction of the hardest constituent. The measured Δj distributions are typically normalized to the total jet number in each p_T interval, constituting a shape-only measurement.

The PYTHIA v8.226 [21] Monte Carlo event generator, configured with the CP5 tune [26] and NNPDF3.1 parton distribution functions at next-to-next-to-leading order [27], is used to simulate particle production in pp collisions. Following the CMS data analysis, final-state jets are reconstructed using the anti-k_T algorithm [28] with a distance parameter of $R = 0.4$, as implemented in the FASTJET framework [23]. To match the acceptance of the experimental work, simulated jets are selected within the kinematic range of $120 < p_T < 300$ GeV and $|\eta| < 1.6$.

In PYTHIA, jets can be identified (or tagged) based on the type of parton originating the shower, allowing differentiation between quark and gluon jets. According to PYTHIA8 simulations, the inclusive jet sample in the transverse momentum range of this study consists of comparable contributions from quark and gluon jets in the absence of medium effects, with the gluon-jet fraction being approximately 53% at $p_T = 120$ GeV and gradually decreasing to about 45% at $p_T = 300$ GeV. The predicted color-charge dependence of partonic energy loss in the presence of QGP is expected to result in a more significant migration of gluon-initiated jets towards lower final-state energy values than quark jets. Since gluon jet Δj distributions are significantly broader than those of quark jets, differences in energy loss (and corresponding migration rates) could also contribute to the narrowing of the jet-axis decorrelations observed in PbPb data by the CMS experiment [19].

Figure 1 shows Δj distributions from PYTHIA simulations. The left panel compares quark- and gluon-initiated jets in the range $230 < p_T < 300$ GeV, with quark jets exhibiting narrower Δj distributions than gluon jets. The right panel illustrates the p_T dependence for inclusive jet distributions, comparing jets with $120 < p_T < 150$ GeV and $230 < p_T < 300$ GeV, indicating narrowing at higher p_T. In both panels, the distributions exhibit stronger shape

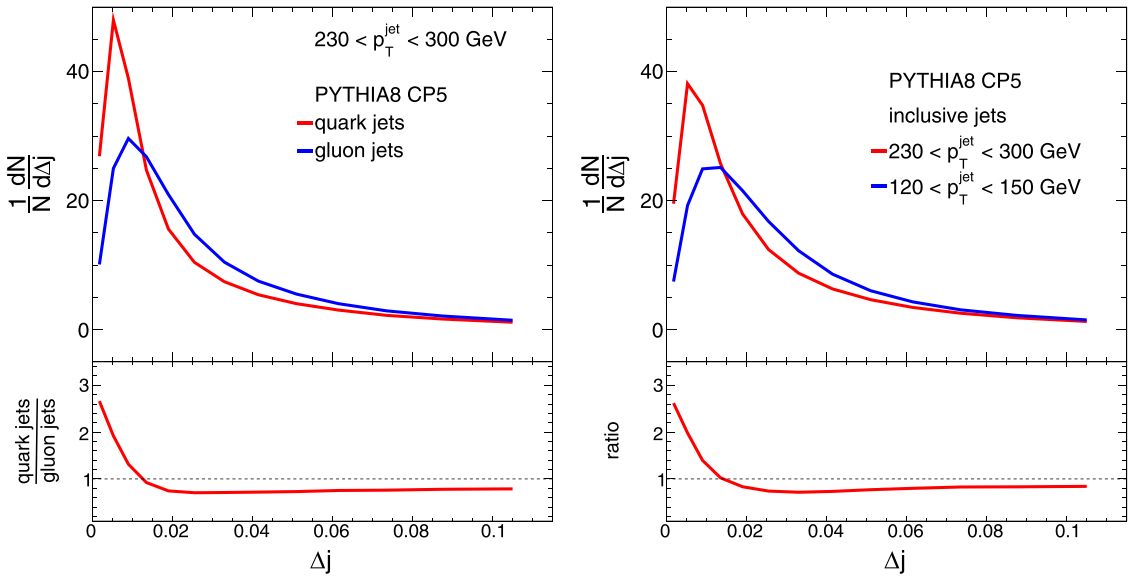


FIG. 1. Left: ΔR_{axis} distributions for quark and gluon jets in PYTHIA8, illustrating flavor dependence. Right: p_{T} dependence of the distribution for inclusive jets. The bottom panel shows the ratio of the distributions.

dependence at small Δj, while at larger Δj, there is little to no difference between quark and gluon jets or across different p_{T} intervals.

A. Template fits

A template fit was performed on the CMS PbPb data using distributions associated with different partons derived from PYTHIA simulations. The primary goal was to investigate a potential shift in the rates between quark and gluon jets. Since PYTHIA is a vacuum-like (unquenched) simulation, this fitting attempt is designed to capture the full extent of the observed modifications in the CMS PbPb data by reducing the relative abundance of gluon jets in the measured inclusive jet sample. All quark flavors are combined into a single quark template and a two-component quark-gluon template fit is applied to each measured CMS distribution. Figure 2 illustrates the template fits for different centrality and jet p_{T} intervals. Centrality is defined as the fraction of the total nucleus-nucleus cross section, with the interval 0–10% corresponding to the sample with the highest average overlap of the colliding nuclei. The fit range is shown in the Δj distributions and the lower panels display the ratio of data to fits.

B. Estimation of energy loss via p_{T} shift for inclusive, quark, and gluon jets

The jets reconstructed experimentally in heavy-ion collisions have been subjected to medium-induced effects (i.e., quenching) and, therefore, the final-state reconstructed energy is expected to be less than that of the parton initiating the jet. Since the jet axis decorrelation observable, Δj, strongly depends on the initial parton p_{T}, the observed narrowing of the distribution could be interpreted as a momentum shift in the reconstructed jet p_{T} due to jet quenching. We investigate this hypothesis by systematically increasing the jet p_{T} in PYTHIA to find the best description of the data without varying the expected quark and gluon jet abundances (the fraction of gluon-initiated jets naturally decreases with jet p_{T} in the kinematic range of this study). The optimal shift is determined by the minimum χ^2 between the p_{T}-shifted PYTHIA-based inclusive jet Δj distributions and the CMS PbPb Δj data across the nominal p_{T} ranges and centrality bins. This procedure involves incrementally increasing the jet p_{T} by $+1$ GeV in the PYTHIA templates at each step. For instance, for inclusive jets in the PbPb data with p_{T} in the range $120 < p_{\text{T}} < 130$ GeV, the corresponding PYTHIA jet p_{T} range is shifted to $121 < p_{\text{T}} < 131$ GeV, $122 < p_{\text{T}} < 132$ GeV, and so on, with the χ^2 value computed at each step.

The results of this study demonstrate that applying a p_{T} shift to the momenta of inclusive jets produces a narrowing of the Δj distributions. While the inclusive p_{T}-shift model exhibits greater tension with the data at low Δj compared with the other methods, it provides a consistently better description in the range $\Delta\text{j} \approx 0.03$–$0.05$, where the other methods show an apparent tension in the two higher jet p_{T} bins (see Fig. 3). Nevertheless, because the data uncertainties increase with Δj, the inclusive p_{T}-shift model shows substantially worse overall agreement with the data in terms of the χ^2 per degree of freedom than that achieved with the two-component fit in central collisions. The average p_{T} shift values, representing the amount of energy lost by the jets, are found to increase with centrality, reaching the largest values in the most central 0–10% collisions. The extracted shift values decrease progressively toward more peripheral collisions. In the 50–80% centrality range, the nominal and shifted p_{T} ranges become nearly identical. Similar trends are observed when allowing for the independent variation of quark- and gluon-initiated jet energies, with gluon jets consistently preferring larger p_{T}-shift values. The average p_{T} shift for inclusive jets (i.e., with identical shifts applied to both the quark and gluon jets), as

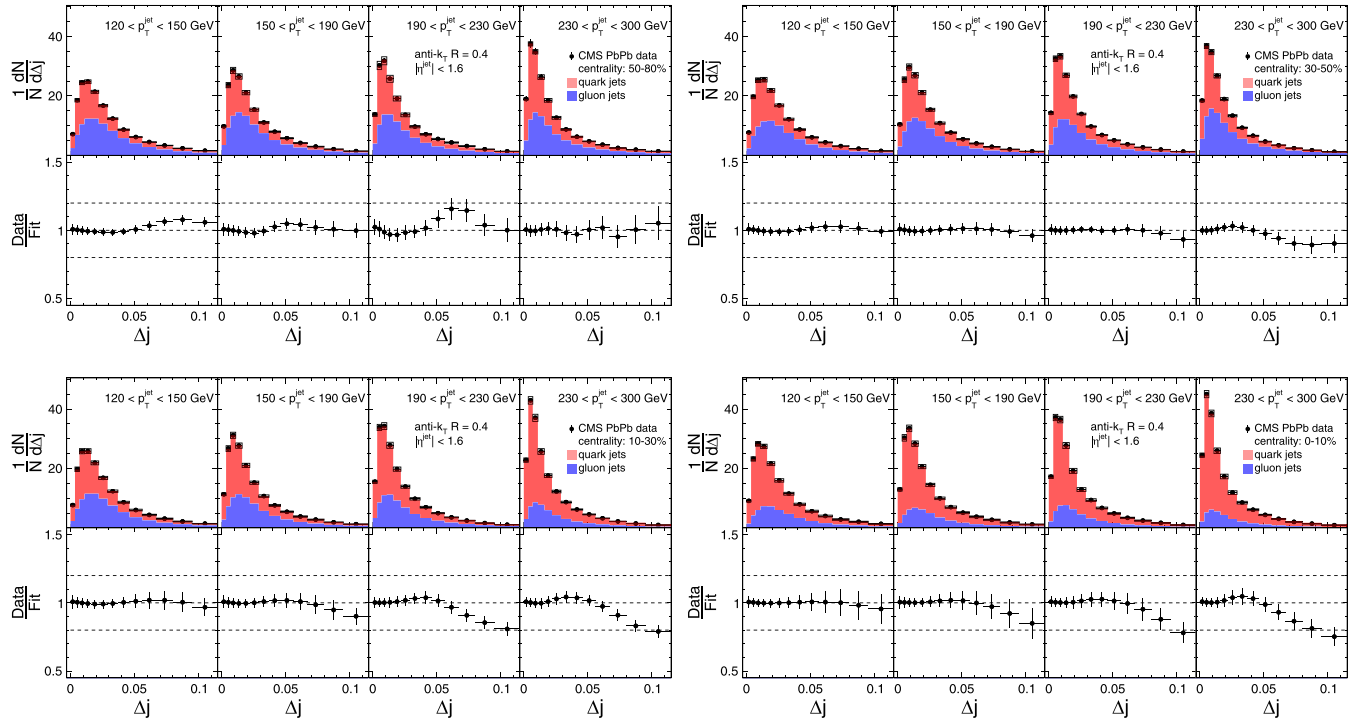


FIG. 2. Template fits to the inclusive jet Δj distributions (black circles) in PbPb collisions for 50–80% (top left), 30–50% (top right), 10–30% (bottom left), and 0–10% (bottom right) centrality intervals, measured by CMS across different p_T intervals. Quark and gluon jet templates from PYTHIA are shown as red and blue shaded areas, respectively. The lower panels show the data-to-fit ratios. Systematic uncertainties in CMS data are represented by rectangles (correlated) and shaded areas (uncorrelated), while vertical solid lines denote statistical uncertainties. In the lower panels, vertical lines represent total data uncertainties.

well as for independently shifted quark- and gluon-initiated jets, is presented in Table I for the 0–10% central collisions, where the greatest energy loss is expected. As anticipated, gluon-initiated jets exhibit a larger p_T shift, consistent with larger energy loss for gluons traversing the medium. These average p_T shifts serve as a quantitative measure of the energy lost by jets during their interactions with the QGP medium.

III. RESULTS AND DISCUSSION

Figure 3 compares the resulting template fit curves (represented by green bands), referred to as the "two-component fit," with the CMS Δj distributions (black circles) for 0–10% centrality across various p_T intervals. The ratios between the CMS data and simulation are displayed in the lower panels. The two-component fits capture the data trends at low p_T, but the fit quality deteriorates in higher p_T bins. It is worth noting that the discrepancies are most pronounced at high Δj values, where little to no shape difference remains between the quark and gluon jet templates. These deviations suggest modifications beyond simple changes in the gluon fraction or simplistic p_T shifts are present in the data that cannot be captured by the vacuum PYTHIA templates.

TABLE I. Summary of the nominal p_T, shifted inclusive p_T, and shifted quark/gluon jet p_T ranges, along with their corresponding means, obtained from the PYTHIA simulation. The shifted p_T ranges and means are determined by minimizing the χ^2 between the Δj distributions from PYTHIA and CMS data in the 0–10% centrality bin.

Nominal p_T (in GeV)	$120 < p_T < 150$	$150 < p_T < 190$	$190 < p_T < 230$	$230 < p_T < 300$
Nominal $\langle p_T \rangle$ (in GeV)	131.98 ± 0.016	165.50 ± 0.02	206.20 ± 0.024	255.50 ± 0.036
Nominal $\langle p_T \rangle$ of quark-like jets (in GeV)	132.11 ± 0.022	165.68 ± 0.028	206.39 ± 0.031	255.81 ± 0.047
Nominal $\langle p_T \rangle$ of gluon-like jets (in GeV)	131.87 ± 0.022	165.32 ± 0.029	205.97 ± 0.035	255.05 ± 0.056
Shifted p_T (in GeV)	$142 < p_T < 172$	$180 < p_T < 220$	$222 < p_T < 262$	$275 < p_T < 345$
Shifted $\langle p_T \rangle$ (in GeV)	154.26 ± 0.017	196.03 ± 0.023	238.58 ± 0.026	301.41 ± 0.042
Shifted p_T of quark-like jets (in GeV)	$123 < p_T < 153$	$150 < p_T < 190$	$192 < p_T < 232$	$230 < p_T < 300$
Shifted $\langle p_T \rangle$ of quark-like jets (in GeV)	135.13 ± 0.023	165.68 ± 0.028	208.41 ± 0.031	255.81 ± 0.047
Shifted p_T of gluon-like jets (in GeV)	$138 < p_T < 168$	$177 < p_T < 217$	$219 < p_T < 259$	$277 < p_T < 347$
Shifted $\langle p_T \rangle$ of gluon-like jets (in GeV)	150.12 ± 0.024	192.85 ± 0.033	235.45 ± 0.039	303.05 ± 0.067

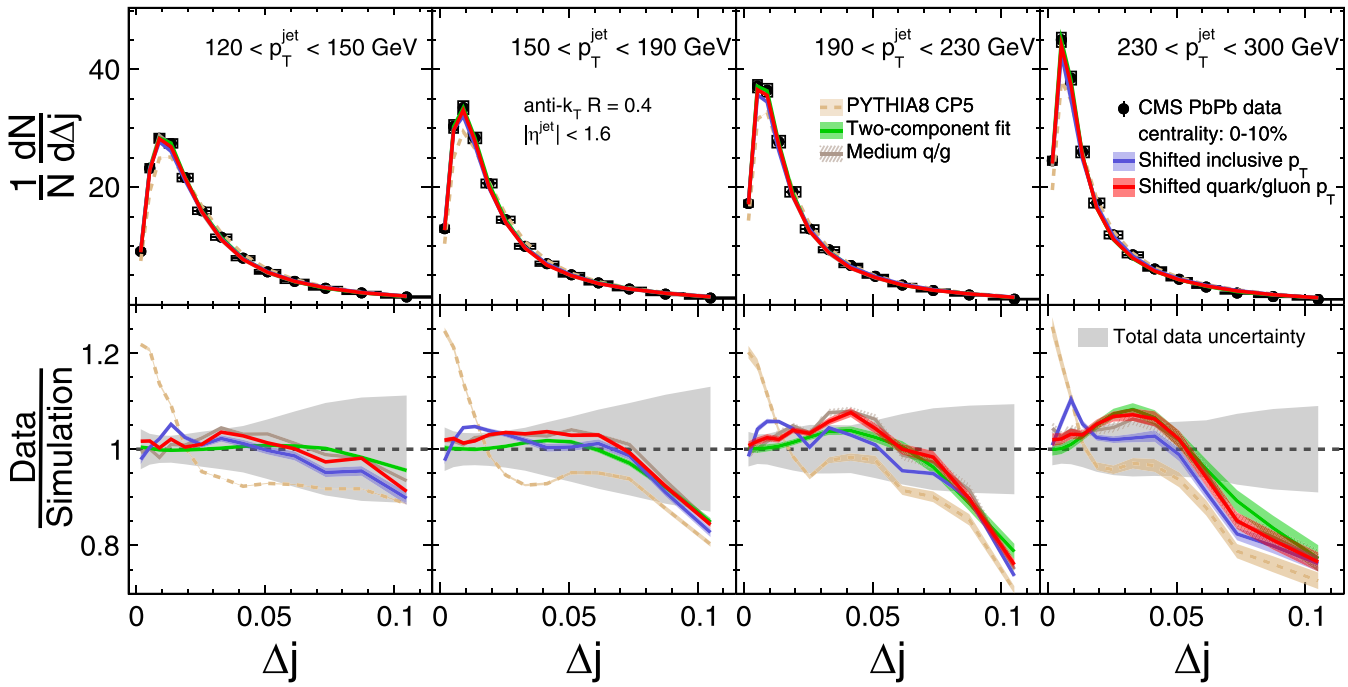


FIG. 3. Normalized Δj distributions from PYTHIA-based simulations using shifted inclusive p_T (blue bands) and shifted quark/gluon p_T (red bands) are compared with CMS unfolded measurements in PbPb collisions at 0–10% centrality (black circles). The results are also compared with unquenched PYTHIA simulations (yellow dashed-line bands), a two-component fit (green bands), and the medium q/g model (hatched lines) across various p_T intervals. Only statistical uncertainties are shown for the simulation distributions. For the CMS data points, systematic uncertainties are indicated by rectangles (correlated uncertainties) and shaded areas (uncorrelated uncertainties), while vertical solid lines depict statistical uncertainties. In the lower panels, the gray bands correspond to the total uncertainties in the data.

The figures also include unquenched PYTHIA distributions (represented by the yellow dashed lines) and the modeling curve based on medium q/g fractions (shown as hatched lines). The unquenched PYTHIA distributions exhibit the largest discrepancies with CMS data. The medium q/g modeling curve is constructed using PYTHIA-based templates with modified quark/gluon fractions, incorporating medium-induced modifications to jet functions [13,19]. This model describes the most central data points (for which predictions were available) across most of the measured Δj range. However, at higher Δj values in the higher p_T bins, the model overestimates the width of the data distributions, even when considering predominantly narrow (quark-initiated) jets in simulation. This observation supports the conclusion that, while the bulk of the distribution is well described, the large-Δj behavior observed in CMS data cannot be explained solely by changes in the quark/gluon composition of the sample. Instead, this discrepancy highlights the need to account for medium-induced substructure modifications to more accurately describe the data.

Using the shifted p_T ranges obtained through minimum χ^2 optimization, we recalculated the Δj distributions in PYTHIA and compared them with the CMS PbPb measurements for 0–10% centrality across four p_T intervals (shown as the blue and red bands in Fig. 3). Similar to the template fit curves, the p_T-shifted distributions align well with peripheral collision data within uncertainties but fail to fully reproduce the features of central collisions, particularly in the higher p_T bins at larger Δj values. Interestingly, the p_T-shifted distributions closely match predictions from the two-component fit and medium q/g models, with better agreement observed for the independent shift scenario.

A. Limits on gluon fraction

The left panel of Fig. 4 shows the extracted best-fit gluon fractions as a function of jet p_T, derived from the template fits to the CMS data, presented earlier (see Fig. 2). Since the template fitting attempts to capture all possible modifications by mere q/g fraction changes, the extracted gluon-like jet fraction values provide the lower bounds for what might be expected from realistic energy loss mechanisms. Any additional mechanisms contributing to the narrowing of the Δj distribution (unrelated to changes in quark and gluon jet abundances due to color-charge effects on energy loss) would likely increase this estimate.

Each variation of the Δj distributions described in Sec. 5 of the CMS paper [19] was used to estimate the systematic uncertainties associated with the extraction of gluon-like jet fractions. For each variation, the modified Δj distribution was fitted and the corresponding gluon-jet fraction was extracted. Deviations from the nominal value were treated as systematic uncertainties. When multiple variations were available for a given source, the largest deviation from the nominal was taken. The total uncertainty was calculated by combining the individual contributions in quadrature.

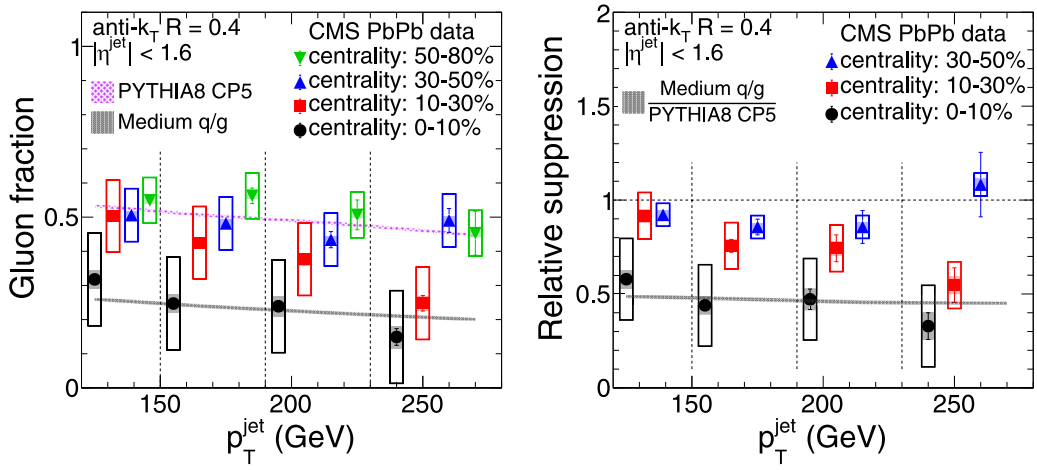


FIG. 4. Left: limits on gluon jet fraction obtained from template fits to the CMS PbPb inclusive Δj measurement using PYTHIA-based templates for the 0–10% (black circles), 10–30% (red squares), 30–50% (blue triangles), and 50–80% (green triangles) centrality intervals. The purple and black bands represent the gluon fraction expectations from the unquenched PYTHIA and medium q/g models, respectively. Right: the ratio of the extracted gluon fraction limits for each centrality interval to those measured in the 50–80% centrality interval is shown. The black band represents the ratio between the expectations from the PYTHIA and medium q/g models. Vertical lines represent statistical uncertainties, while systematic uncertainties are shown as rectangles (correlated uncertainties) and shaded areas (uncorrelated uncertainties). Points in each jet p_T bin are shifted horizontally for better visibility.

The right panel of Fig. 4 presents the ratio of the gluon fraction limits for each centrality interval relative to those in the 50–80% centrality range, emphasizing the centrality-dependent evolution of the observed variations. A lower limit on the gluon fractions is obtained for more central events, particularly at higher transverse momenta. This trend is more apparent in the ratio of the limits, where gluon-like jet fraction is reduced by approximately 50% for 0–10% central events. We find that the estimated gluon fraction from template fitting to the Δj distributions is in agreement with the predictions from the medium q/g model for 0–10% central collisions [13,19].

B. Calculation of jet R_{AA} using shifted p_T

To further explore the applicability of the p_T shift estimates for jet quenching modeling, we construct a jet R_{AA} estimate by dividing the jet counts in the shifted p_T ranges by those in the corresponding nominal p_T ranges in PYTHIA. For the quark and gluon jet p_T shifts, jets were first counted separately for each jet type, then combined, and the resulting counts were divided by those from the nominal p_T ranges. The jet R_{AA} estimate constructed using the inclusive jet p_T shift is expected to provide a lower limit, while modeling the individual shifts to quark and gluon jet energies offers a more realistic estimate of energy loss. The resulting R_{AA} estimates, shown in the left panel of Fig. 5, are presented for both the inclusive jet p_T shift and the independent quark/gluon jet p_T shifts. The uncertainty on the R_{AA} estimate is quantified by varying the p_T shifts by minimizing $\chi^2 + 1$ and then calculating the difference between the resulting values. Remarkably, the constructed jet R_{AA} estimates for both types of energy loss modeling align closely with previously measured jet R_{AA} from the CMS and ATLAS experiments [5,29,30]. The agreement of the estimated quenching strength determined in this study, based on the jet axis decorrelation distributions, with earlier jet R_{AA} measurements provides support for the plausibility of the approach developed. The proposed studies of jet-axis-based substructure observables can thus offer additional constraints on medium-induced quark/gluon jet fraction modifications, leading to a more accurate assessment of energy loss in the medium.

C. Average fractional transverse momentum loss ($\langle \Delta p_T \rangle / p_T$)

Alongside the R_{AA} estimates, we also present the average fractional transverse momentum loss, $\langle \Delta p_T \rangle / p_T$, separately for quark and gluon jets, based on the p_T shift values extracted for central 0–10% PbPb collisions, as summarized in Table I. The uncertainties on these values were estimated in the same manner as described earlier: by minimizing $\chi^2 + 1$ and calculating the difference between the resulting values. The calculated $\langle \Delta p_T \rangle / p_T$ as a function of p_T is shown in the right panel of Fig. 5. The results closely align with those reported in Ref. [14], which employed a Bayesian analysis of multiple measurements across the studied p_T ranges.

IV. SUMMARY

This paper presents a phenomenological study of jet axis decorrelation (Δj) between two types of jet axes for inclusive jets from lead-lead (PbPb) collisions at a center-of-mass energy of 5.02 TeV previously measured by the CMS experiment for different centrality selections and jet transverse momentum (p_T) intervals. The fits to these distributions are performed using templates generated with the PYTHIA8 event generator for gluon-initiated jets and jets from quarks of different flavors, attempting to understand the nature of the Δj modifications observed.

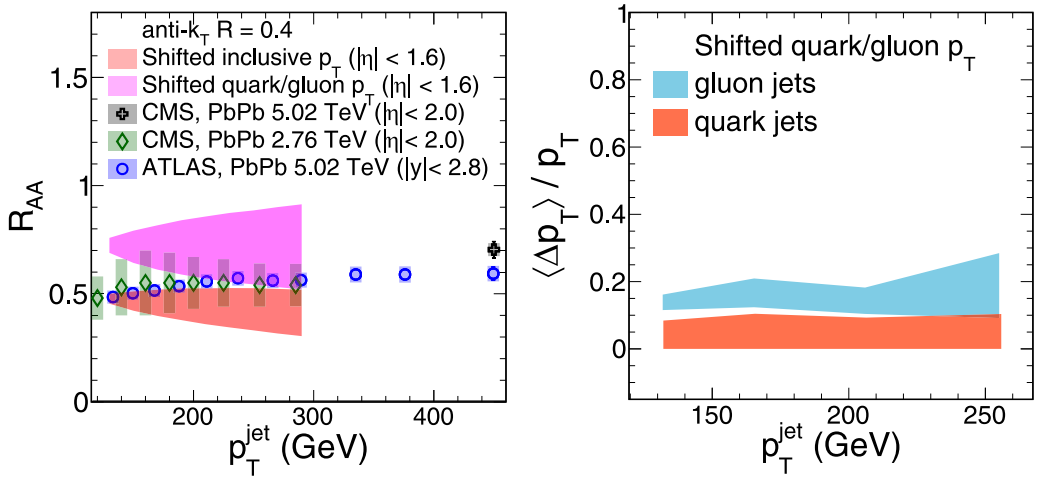


FIG. 5. Left: the jet R_{AA} estimates based on inclusive jet p_T shifts along with the quark and gluon jet p_T shift values extracted from template fits in this analysis are shown alongside other measurements and predictions (see text), for 0–10% centrality. Right: the average fractional transverse momentum loss of quark and gluon jets, determined from the p_T shift values extracted for 0–10% PbPb collisions.

The study is based on anti-k_T jets with a radius parameter $R = 0.4$ across four transverse momentum (p_T) intervals ranging from 120 to 300 GeV within pseudorapidity $|\eta| < 1.6$.

It is found that the (unquenched) PYTHIA8 predictions describe the peripheral CMS PbPb data but fail to capture the distributions from central events, due to the progressive narrowing of the Δj distributions observed toward more central collisions. Limits on possible variations in the jet sample composition were determined using PYTHIA-based two-component template fits to the CMS PbPb data. The fits result in a reduced fraction of gluon jets in the inclusive jet sample studied by CMS, with the most significant reduction observed for the highest-p_T jets in the most central events. This observation is consistent with the expected higher in-medium energy loss of gluon-initiated jets compared to those originating from hard-scattered quarks.

Furthermore, two possible scenarios of jet energy loss were investigated using transverse momentum shifted selections of jets in MC samples. First, an inclusive p_T shift was applied to all jets (regardless of flavor) and then differences in energy loss between quarks and gluons were probed by independently shifting the momenta of quark- and gluon-initiated jets in PYTHIA8 simulations. The study was performed for the most central CMS data, where medium-induced modification to the jet-axis decorrelation distributions is most significant. The results of the inclusive p_T-shift study do not provide the best description of the measured distributions, indicating a disfavoring of a common energy loss scenario. The results of the independent quark- and gluon-jet energy variations study indicate a higher energy loss for gluon jets compared to quark jets, consistent with theoretical expectations. The extracted p_T shifts corresponding to the best description of the jet substructure data provide estimates of flavor-dependent energy loss as a function of jet p_T. The gluon jet fractions extracted from this approach are found to be reduced by amounts similar to those from the vacuum expectations as estimated from the two-component fit. To further assess the plausibility of our approach and assumptions, these p_T shifts derived from CMS central PbPb collision data, the corresponding estimate for a jet nuclear modification factor R_{AA} was calculated and shown to be consistent with the measured jet R_{AA}, providing a coherent jet quenching picture. Finally, the average fractional transverse momentum loss for jets initiated by different partons was calculated and compared with previous experimental and theoretical results.

The study presented in this work illustrates the use of the jet substructure observable to study jet quenching mechanisms in greater detail than afforded by the inclusive-type measurements. The extracted limits on changes in the gluon-initiated jet fraction, along with estimates of quark and gluon jet energy loss in the studied kinematic range, provide new constraints on the color-charge dependence of energy loss and offer valuable insights for jet quenching models.

ACKNOWLEDGMENTS

The authors acknowledge A. Baty, H. Bossi, M. Calderon De La Barca, P. Maksimovic, S. Salur, and L. Cunqueiro Mendez for useful discussions and input during the development of this work. The authors thank F. Ringer and N. Sato for providing the data points for Ref. [13]. This work is supported by the U.S. Department of Energy, Grant No. DE-FG02-94ER40865.

DATA AVAILABILITY

The data that support the findings of this article are not publicly available. The data are available from the authors upon reasonable request.

[1] L. Apolinário, Y.-J. Lee, and M. Winn, Heavy quarks and jets as probes of the QGP, Prog. Part. Nucl. Phys. **127**, 103990 (2022).

[2] L. Cunqueiro and A. M. Sickles, Studying the QGP with jets at the LHC and RHIC, Prog. Part. Nucl. Phys. **124**, 103940 (2022).

[3] K. Adcox, *et al.* (PHENIX Collaboration), Suppression of hadrons with large transverse momentum in central Au+Au collisions at $\sqrt{s_{\rm NN}} = 130$ GeV, Phys. Rev. Lett. **88**, 022301 (2001).

[4] C. Adler, *et al.* (STAR Collaboration), Centrality dependence of high $p_{\rm T}$ hadron suppression in Au+Au collisions at $\sqrt{s_{\rm NN}} =$ 130 GeV, Phys. Rev. Lett. **89**, 202301 (2002).

[5] A. M. Sirunyan, *et al.* (CMS Collaboration), First measurement of large area jet transverse momentum spectra in heavy-ion collisions, J. High Energy Phys. 05 (2021) 284.

[6] A. M. Sirunyan, *et al.* (CMS Collaboration), In-medium modification of dijets in PbPb collisions at $\sqrt{s_{\rm NN}} = 5.02$ TeV, J. High Energy Phys. 05 (2021) 116.

[7] G. Aad, *et al.* (ATLAS Collaboration), Measurement of suppression of large-radius jets and its dependence on substructure in Pb+Pb collisions at $\sqrt{s_{\rm NN}} = 5.02$ TeV with the ATLAS detector, Phys. Rev. Lett. **131**, 172301 (2023).

[8] S. Acharya, *et al.* (ALICE Collaboration), Measurement of the radius dependence of charged-particle jet suppression in Pb–Pb collisions at $\sqrt{s_{\rm NN}} = 5.02$ TeV, Phys. Lett. B **849**, 138412 (2024).

[9] A. Hayrapetyan, *et al.* (CMS Collaboration), Overview of high-density QCD studies with the CMS experiment at the LHC, Phys. Rep. **1115**, 219 (2025).

[10] S. Acharya, *et al.* (ALICE Collaboration), The ALICE experiment: A journey through QCD, Eur. Phys. J. C **84**, 813 (2024).

[11] R. Kogler, *et al.*, Jet substructure at the large Hadron collider: Experimental review, Rev. Mod. Phys. **91**, 045003 (2019).

[12] R. Vertesi (ATLAS, CMS, and ALICE Collaborations), Jet substructure measurements in heavy-ion collisions, Int. J. Mod. Phys. A **40**, 2444002 (2025).

[13] J.-W. Qiu, F. Ringer, N. Sato, and P. Zurita, Factorization of jet cross sections in heavy-ion collisions, Phys. Rev. Lett. **122**, 252301 (2019).

[14] W.-J. Xing, S. Cao, and G.-Y. Qin, Flavor hierarchy of parton energy loss in quark-gluon plasma from a Bayesian analysis, Phys. Lett. B **850**, 138523 (2024).

[15] S.-L. Zhang, E. Wang, H. Xing, and B.-W. Zhang, Flavor dependence of jet quenching in heavy-ion collisions from a Bayesian analysis, Phys. Lett. B **850**, 138549 (2024).

[16] S. Acharya, *et al.* (ALICE Collaboration), Exploration of jet substructure using iterative declustering in pp and Pb–Pb collisions at LHC energies, Phys. Lett. B **802**, 135227 (2020).

[17] A. M. Sirunyan, *et al.* (CMS Collaboration), Measurement of quark- and gluon-like jet fractions using jet charge in Pb–Pb and pp collisions at 5.02 TeV, J. High Energy Phys. 07 (2020) 115.

[18] G. Aad, *et al.* (ATLAS Collaboration), Comparison of inclusive and photon-tagged jet suppression in 5.02 TeV Pb+Pb collisions with ATLAS, Phys. Lett. B **846**, 138154 (2023); **858**, 138998(E) (2024).

[19] V. Chekhovsky, *et al.* (CMS Collaboration), Search for medium effects using jet axis decorrelation in inclusive jets from Pb–Pb collisions at $\sqrt{s_{\rm NN}} = 5.02$ TeV, J. High Energy Phys. 06 (2025) 120.

[20] P. Cal, D. Neill, F. Ringer, and W. J. Waalewijn, Calculating the angle between jet axes, J. High Energy Phys. 04 (2020) 211.

[21] T. Sjöstrand, S. Ask, J. R. Christiansen, R. Corke, N. Desai, P. Ilten, S. Mrenna, S. Prestel, C. O. Rasmussen, and P. Z. Skands, An introduction to PYTHIA 8.2, Comput. Phys. Commun. **191**, 159 (2015).

[22] V. Khachatryan, *et al.* (CMS Collaboration), Development and validation of HERWIG 7 tunes from CMS underlying-event measurements, Eur. Phys. J. C **81**, 312 (2021).

[23] M. Cacciari, G. P. Salam, and G. Soyez, FastJet user manual, Eur. Phys. J. C **72**, 1896 (2012).

[24] D. Bertolini, T. Chan, and J. Thaler, Jet observables without jet algorithms, J. High Energy Phys. 04 (2014) 013.

[25] A. J. Larkoski, D. Neill, and J. Thaler, Jet shapes with the broadening axis, J. High Energy Phys. 04 (2014) 017.

[26] A. M. Sirunyan, *et al.* (CMS Collaboration), Extraction and validation of a new set of CMS PYTHIA8 tunes from underlying-event measurements, Eur. Phys. J. C **80**, 4 (2020).

[27] R. D. Ball, *et al.* (NNPDF Collaboration), Parton distributions from high-precision collider data, Eur. Phys. J. C **77**, 663 (2017).

[28] M. Cacciari, G. P. Salam, and G. Soyez, The anti-k_T jet clustering algorithm, J. High Energy Phys. 04 (2008) 063.

[29] V. Khachatryan, *et al.* (CMS Collaboration), Measurement of inclusive jet cross sections in pp and Pb–Pb collisions at $\sqrt{s_{\rm NN}} = 2.76$ TeV, Phys. Rev. C **96**, 015202 (2017).

[30] M. Aaboud, *et al.* (ATLAS Collaboration), Measurement of the nuclear modification factor for inclusive jets in Pb+Pb collisions at $\sqrt{s_{\rm NN}} = 5.02$ TeV with the ATLAS detector, Phys. Lett. B **790**, 108 (2019).